

 Open access • Journal Article • DOI:10.1038/NN1302

## **Abeta is targeted to the vasculature in a mouse model of hereditary cerebral hemorrhage with amyloidosis. — Source link**

Martin C. Herzig, David T. Winkler, Patrick Burgermeister, Michelle Pfeifer ...+14 more authors

**Institutions:** University of Tübingen, University of Basel, New York University, Novartis ...+2 more institutions

**Published on:** 15 Aug 2004 - Nature Neuroscience (Nature Publishing Group)

**Topics:** Cerebral amyloid angiopathy, Hereditary cerebral hemorrhage with amyloidosis, Senile plaques, Biochemistry of Alzheimer's disease and P3 peptide

Related papers:

- [Correlative Memory Deficits, A \$\beta\$  Elevation, and Amyloid Plaques in Transgenic Mice](#)
- [Neuronal overexpression of mutant amyloid precursor protein results in prominent deposition of cerebrovascular amyloid](#)
- [Two amyloid precursor protein transgenic mouse models with Alzheimer disease-like pathology](#)
- [Mutation of the Alzheimer's disease amyloid gene in hereditary cerebral hemorrhage, Dutch type.](#)
- [Alzheimer-type neuropathology in transgenic mice overexpressing V717F beta-amyloid precursor protein.](#)

Share this paper:    

View more about this paper here: <https://typeset.io/papers/abeta-is-targeted-to-the-vasculature-in-a-mouse-model-of-epstspby32>



University of Zurich  
Zurich Open Repository and Archive

Winterthurerstr. 190  
CH-8057 Zurich  
<http://www.zora.uzh.ch>

---

*Year: 2004*

---

## Abeta is targeted to the vasculature in a mouse model of hereditary cerebral hemorrhage with amyloidosis

Herzig, M C; Winkler, D T; Burgermeister, P; Pfeifer, M; Kohler, E; Schmidt, S D; Danner, S; Abramowski, D; Stürchler-Pierrat, C; Bürki, K; van Duinen, S G; Maat-Schieman, M L C; Staufenbiel, M; Mathews, P M; Jucker, M

Herzig, M C; Winkler, D T; Burgermeister, P; Pfeifer, M; Kohler, E; Schmidt, S D; Danner, S; Abramowski, D; Stürchler-Pierrat, C; Bürki, K; van Duinen, S G; Maat-Schieman, M L C; Staufenbiel, M; Mathews, P M; Jucker, M (2004). Abeta is targeted to the vasculature in a mouse model of hereditary cerebral hemorrhage with amyloidosis. *Nature Neuroscience*, 7(9):954-60.

Postprint available at:  
<http://www.zora.uzh.ch>

Posted at the Zurich Open Repository and Archive, University of Zurich.  
<http://www.zora.uzh.ch>

Originally published at:  
*Nature Neuroscience* 2004, 7(9):954-60.

# Abeta is targeted to the vasculature in a mouse model of hereditary cerebral hemorrhage with amyloidosis

## Abstract

The E693Q mutation in the amyloid beta precursor protein (APP) leads to cerebral amyloid angiopathy (CAA), with recurrent cerebral hemorrhagic strokes and dementia. In contrast to Alzheimer disease (AD), the brains of those affected by hereditary cerebral hemorrhage with amyloidosis-Dutch type (HCHWA-D) show few parenchymal amyloid plaques. We found that neuronal overexpression of human E693Q APP in mice (APPDutch mice) caused extensive CAA, smooth muscle cell degeneration, hemorrhages and neuroinflammation. In contrast, overexpression of human wild-type APP (APPwt mice) resulted in predominantly parenchymal amyloidosis, similar to that seen in AD. In APPDutch mice and HCHWA-D human brain, the ratio of the amyloid-beta40 peptide (Abeta40) to Abeta42 was significantly higher than that seen in APPwt mice or AD human brain. Genetically shifting the ratio of AbetaDutch40/AbetaDutch42 toward AbetaDutch42 by crossing APPDutch mice with transgenic mice producing mutated presenilin-1 redistributed the amyloid pathology from the vasculature to the parenchyma. The understanding that different Abeta species can drive amyloid pathology in different cerebral compartments has implications for current anti-amyloid therapeutic strategies. This HCHWA-D mouse model is the first to develop robust CAA in the absence of parenchymal amyloid, highlighting the key role of neuronally produced Abeta to vascular amyloid pathology and emphasizing the differing roles of Abeta40 and Abeta42 in vascular and parenchymal amyloid pathology.

# A $\beta$ is targeted to the vasculature in a mouse model of hereditary cerebral hemorrhage with amyloidosis

Martin C Herzig<sup>1,2</sup>, David T Winkler<sup>2</sup>, Patrick Burgermeister<sup>2</sup>, Michelle Pfeifer<sup>1,2</sup>, Esther Kohler<sup>1,2</sup>, Stephen D Schmidt<sup>3</sup>, Simone Danner<sup>4</sup>, Dorothee Abramowski<sup>4</sup>, Christine Stürchler-Pierrat<sup>4</sup>, Kurt Bürki<sup>5</sup>, Sjoerd G van Duinen<sup>6</sup>, Marion L C Maat-Schieman<sup>6</sup>, Matthias Staufenbiel<sup>4</sup>, Paul M Mathews<sup>3</sup> & Mathias Jucker<sup>1,2</sup>

The E693Q mutation in the amyloid beta precursor protein (APP) leads to cerebral amyloid angiopathy (CAA), with recurrent cerebral hemorrhagic strokes and dementia. In contrast to Alzheimer disease (AD), the brains of those affected by hereditary cerebral hemorrhage with amyloidosis–Dutch type (HCHWA-D) show few parenchymal amyloid plaques. We found that neuronal overexpression of human E693Q APP in mice (APPDutch mice) caused extensive CAA, smooth muscle cell degeneration, hemorrhages and neuroinflammation. In contrast, overexpression of human wild-type APP (APPwt mice) resulted in predominantly parenchymal amyloidosis, similar to that seen in AD. In APPDutch mice and HCHWA-D human brain, the ratio of the amyloid- $\beta$ 40 peptide (A $\beta$ 40) to A $\beta$ 42 was significantly higher than that seen in APPwt mice or AD human brain. Genetically shifting the A $\beta$ Dutch40/A $\beta$ Dutch42 ratio toward A $\beta$ Dutch42 by crossing APPDutch mice with transgenic mice producing mutated presenilin-1 redistributed the amyloid pathology from the vasculature to the parenchyma. The understanding that different A $\beta$  species can drive amyloid pathology in different cerebral compartments has implications for current anti-amyloid therapeutic strategies. This HCHWA-D mouse model is the first to develop robust CAA in the absence of parenchymal amyloid, highlighting the key role of neuronally produced A $\beta$  to vascular amyloid pathology and emphasizing the differing roles of A $\beta$ 40 and A $\beta$ 42 in vascular and parenchymal amyloid pathology.

Mutations in APP at the  $\beta$ - and  $\gamma$ -secretase sites have been shown to cause familial forms of early-onset AD. These mutations increase the production of either total amyloid- $\beta$  peptides (A $\beta$ ) or the more amyloidogenic A $\beta$ 1–42 species. In contrast, most mutations within the A $\beta$  domain do not result in a full range of AD pathology but characteristically result in cerebrovascular pathology<sup>1–3</sup>. For example, the E693Q point mutation in APP (affecting residue 22 of A $\beta$ ) results in HCHWA-D, an autosomal-dominant form of CAA<sup>4,5</sup>. Those afflicted with HCHWA-D suffer from recurrent lobar cerebral hemorrhages, with an onset in the fifth decade of life<sup>6</sup>. At autopsy, extensive CAA is typically found in leptomeningeal arteries and cortical arterioles, and to a lesser extent in meningeal veins. Unlike in AD, parenchymal amyloid plaques are not prominent in HCHWA-D, although diffuse parenchymal A $\beta$  is found<sup>7</sup>. Because of these features of the disease, HCHWA-D has become the human genetic archetype of the A $\beta$  congophilic angiopathy seen sporadically in many of the elderly and in the majority of those with AD<sup>8,9</sup>.

Previous *in vitro* findings have shown that A $\beta$  harboring the Dutch E693Q mutation (A $\beta$ Dutch) has been associated with enhanced aggregation properties, reduced clearance from the brain and greater toxicity in smooth muscle cells, as compared to wild-type A $\beta$

(A $\beta$ wt)<sup>10–14</sup>. However, the reasons for the predominant cerebral vascular amyloid deposition in HCHWA-D are unclear. In the present study, we generated human APP E693Q transgenic mice (APPDutch mice) to study the mechanisms underlying vascular amyloidosis and the consequences of CAA using an *in vivo* model system.

## RESULTS

### A $\beta$ 1–40 predominates in vascular amyloid in HCHWA-D

Cerebrovascular amyloid in human HCHWA-D postmortem brain tissue was found predominantly in the leptomeningeal and cortical vessel walls, often with limited labeling of diffuse parenchymal A $\beta$  deposits (Fig. 1a). Immunohistochemical staining with C terminus-specific antibodies to A $\beta$  suggest that A $\beta$ 40 predominates over A $\beta$ 42 in the cerebrovascular amyloid (Fig. 1b,c). To confirm this and to determine whether A $\beta$ Dutch is the predominant A $\beta$  species deposited in the vessel wall, we used bicine/Tris/urea SDS-PAGE<sup>15</sup> to separate various A $\beta$  species. Both HCHWA-D cortical tissue and isolated leptomeningeal vessels contained abundant A $\beta$ Dutch1–40 as well as substantial amounts of A $\beta$ wt1–40 (Fig. 1d). In contrast, in the brains of individuals with sporadic AD, both A $\beta$ 1–40 and A $\beta$ 1–42 were present (Fig. 1d). These observations were confirmed

<sup>1</sup>Department of Cellular Neurology, Hertie-Institute for Clinical Brain Research, University of Tübingen, D-72076 Tübingen, Germany. <sup>2</sup>Department of Neuropathology, Institute of Pathology, University of Basel, CH-4003 Basel, Switzerland. <sup>3</sup>Nathan Kline Institute, New York University School of Medicine, Orangeburg, New York 10962, USA. <sup>4</sup>Novartis Institutes for Biomedical Research, Nervous Systems Research, CH-4002 Basel, Switzerland. <sup>5</sup>Institute of Laboratory Animal Science, University of Zürich, CH-8057 Zürich, Switzerland. <sup>6</sup>Departments of Pathology and Neurology, Leiden University Medical Center, 2300 RC Leiden, The Netherlands. Correspondence should be addressed to M.J. (mathias.jucker@uni-tuebingen.de).

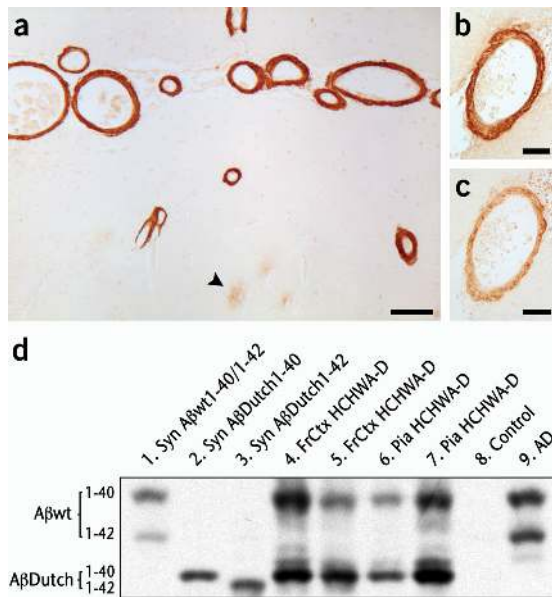


**Figure 1** Vascular amyloid in HCHWA-D brain consists of both A $\beta$ Dutch and A $\beta$ wt, with A $\beta$ 1–40 being the predominant peptide. **(a)** Frontal cortex of the brain of an individual (50 years of age) with HCHWA-D immunostained with antibody NT12 to A $\beta$ . Massive amyloid deposition within leptomeningeal and cortical vessel walls is observed. Only few and diffuse parenchymal A $\beta$  deposits are visible (arrowhead), although pretreatment may increase parenchymal staining<sup>50</sup>. **(b, c)** Immunolabeling of vascular amyloid with antibodies specific to A $\beta$ x–40 (R208 in **b**) and A $\beta$ x–42 (R306 in **c**) reveals that the majority of vascular amyloid ends at amino acid 40. **(d)** Western blotting of brain homogenates. Synthetic A $\beta$  is shown in lanes 1–3. Homogenates of frontal cortex (lanes 4 and 5) and pia (lanes 6 and 7) of HCHWA-D patients contain both A $\beta$ wt1–40 and A $\beta$ Dutch1–40, but no detectable A $\beta$ wt1–42 or A $\beta$ Dutch1–42. This observation suggests that cerebrovascular amyloid in HCHWA-D patients consists of both A $\beta$ wt and A $\beta$ Dutch and is predominantly of the A $\beta$ 1–40 isoform. Control individuals showed no detectable A $\beta$  (lane 8), whereas both A $\beta$ wt1–40 and 1–42 were found in patients with sporadic AD patients (lane 9). Scale bars are 100  $\mu$ m (**a**) and 50  $\mu$ m (**b, c**).

by ELISA, which showed only half as much A $\beta$ 40 as A $\beta$ 42 in AD brain tissue, and 18 times more A $\beta$ 40 than A $\beta$ 42 in HCHWA-D brain tissue (Table 1).

### Neuronal overexpression of human E693Q APP leads to CAA

To understand the pathogenesis of HCHWA-D and the mechanisms leading to cerebrovascular amyloid, we generated transgenic mice (APPDutch mice) overexpressing E693Q-mutated human APP (hAPP) under the control of the neuron-specific Thy1 promoter element. High levels of hAPP mRNA were detected in neocortex, hippocampus and brain stem by *in situ* hybridization (Fig. 2a). Consistently, immunohistochemistry revealed robust hAPP expression in the same brain regions, exclusively within neurons and neuronal processes. No hAPP mRNA or protein was detected in vessel walls (Fig. 2b). We selected two transgenic lines with high hAPP expression levels that remained constant with aging (Fig. 2c). By direct western blot analysis, A $\beta$ Dutch could not be detected in young APPDutch mice. A $\beta$ Dutch1–40, however, was readily detectable in a 23-month-old mouse, consistent with amyloid deposition at this age (Fig. 2c). Morphological analysis of APPDutch mice between 22 and 30 months of age ( $n = 30$ ) showed an onset of vascular amyloid deposition at approximately 22–25 months for both lines. Amyloid deposition in the brain was largely confined to the cerebral vasculature (Fig. 2d), appearing

**Table 1** A $\beta$ 40/A $\beta$ 42 ratios in brains of transgenic mice and humans with HCHWA-D and AD

	Human A $\beta$ 40/A $\beta$ 42		Murine A $\beta$ 40/A $\beta$ 42
	Predepositing	Depositing	Depositing
APPwt	4.3 $\pm$ 0.3	2.8 $\pm$ 0.4	1.1 $\pm$ 0.1
APPDutch	7.8 $\pm$ 0.9**	12.1 $\pm$ 1.4***	3.0 $\pm$ 0.5**
APPDutch/PS45	0.4 $\pm$ 0.9	0.4 $\pm$ 0.02	
HCHWA-D		18.6 $\pm$ 7.0	
AD		0.5 $\pm$ 0.19	

Levels of human and murine A $\beta$ 40 and A $\beta$ 42 were determined by ELISA in A $\beta$ -depositing 18-month-old APPwt mice and 28-month-old APPDutch mice ( $n = 5–11$ ). Human A $\beta$  was measured in predepositing 7-month-old APPwt and APPDutch mice ( $n = 6–9$ ), in predepositing 3-month-old and A $\beta$ -depositing 9-month-old APPDutch/PS45 mice, and in AD and HCHWA-D patients ( $n = 3–9$ ). Data are the means of the individual A $\beta$ 40/A $\beta$ 42 ratios  $\pm$  s.e.m. \*\* $P < 0.01$ , \*\*\* $P < 0.001$  (comparison with APPwt). Absolute A $\beta$  values are reported in **Supplementary Table 1** online.

first in leptomeningeal vessels followed by cortical vessels. Female mice seemed to have an earlier onset than males. Similar to human HCHWA-D brain tissue and consistent with the western blot analysis, immunoreactivity for A $\beta$ 40 was much more intense than for A $\beta$ 42 (Fig. 2e,f). Congo red (Fig. 2g) and Thioflavin S staining (data not shown) demonstrated that much of the cerebrovascular amyloid was in a compact  $\beta$ -pleated sheet conformation. Some amyloid-laden vessels showed a vessel-within-vessel configuration (Fig. 2h). With an electron microscope, we observed an irregular thickening of the basement membrane with amorphous material in some vessels, whereas others contained amyloid fibrils within the basement membrane—predominantly on the adventitial side—and the endothelial cell layer appeared to be intact. At a more advanced stage, amyloid fibrils were observed in a radial pattern between the smooth muscle cells, with some fibrils invading the parenchyma (Fig. 2i). Despite a substantial vascular amyloid burden, APPDutch mice did not develop compact parenchymal amyloid plaques and only rarely were diffuse parenchymal A $\beta$  deposits observed.

### CAA induces hemorrhages and neuroinflammation

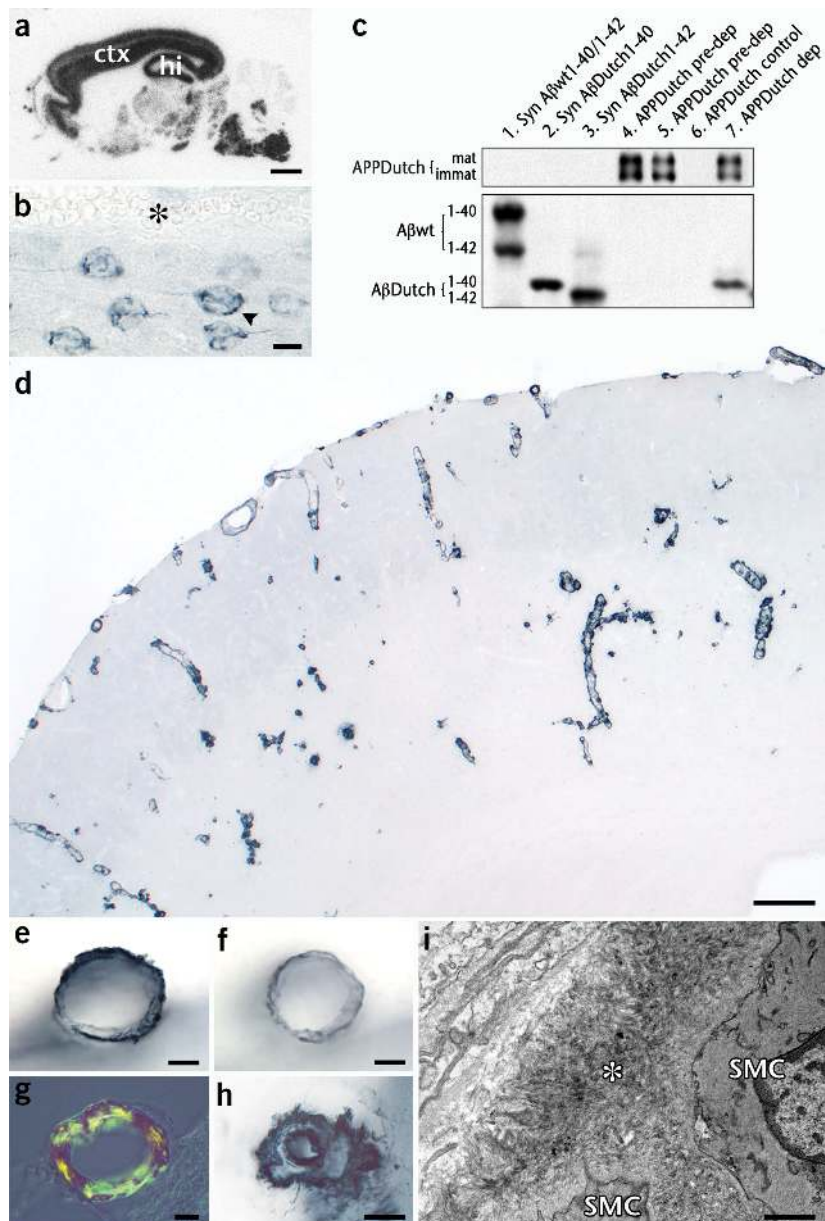
Amyloid-laden vessels in APPDutch mice show a severe loss of smooth muscle cells (Fig. 3a,b). Consistent with the loss of smooth muscle cells and a concomitant weakening of the vessel walls, fresh hemorrhages (Fig. 3c,d), as well as indications of previous hemorrhages (Fig. 3e,f), were found in three of the oldest APPDutch mice. No bleeding was found in age-matched, nontransgenic mice (data not shown).

In APPDutch mice with CAA, a strong, perivascular microglial inflammatory reaction was observed (Fig. 3g). This microgliosis was confined to the immediate vicinity of amyloid-laden vessels and was absent in locations adjacent to unaffected vessels (Fig. 3h). In addition, an activation of astrocytes was observed throughout all neocortical areas affected by CAA (Fig. 3i) but not in brain areas devoid of vascular amyloid and in nontransgenic control mice (Fig. 3j). The widespread astrocytosis in areas affected with CAA may be the result of partial ischemia and a perfusion deficit associated with amyloid-laden vessels.

### Increased A $\beta$ 40/A $\beta$ 42 ratio in APPDutch versus APPwt mice

To examine the determinants that lead to vascular versus parenchymal amyloid deposition, we compared the pattern of amyloid deposition in APPDutch mice with that of transgenic mice overexpressing wild-type hAPP at levels similar to the APPDutch mice, under the control of the same Thy1 promoter element and in the same C57BL/6J genetic background (APPwt mice). Aged APPwt mice developed parenchymal plaques with limited vascular deposits (Fig. 4a). Western blot analysis of APPwt mice with amyloid

**Figure 2** APPDutch mice develop cerebral amyloid angiopathy. (a) *In situ* hybridization reveals high transgene-derived mRNA levels in neocortex (ctx) and hippocampus (hi) and brain stem. (b) Immunostaining for hAPP in neocortex shows punctate labeling of neuronal perikarya (arrowhead) and weaker labeling of axonal processes. Consistent with the neuron-specific promoter, there was no hAPP expression in the vessel wall (the lumen of the vessel is indicated by an asterisk). (c) Western blot analysis of hAPP and hA $\beta$  in mouse brain using an antibody specific to human APP/A $\beta$ . Upper panel: APPDutch expression in APPDutch mouse lines 23 (lane 4) and 33 (lanes 5 and 7) and a nontransgenic control littermate (lane 6). Bands demonstrate immature and mature forms of hAPP. Lower panel: synthetic human A $\beta$ wt1–40 mixed with human A $\beta$ wt1–42, A $\beta$ Dutch1–40 and A $\beta$ Dutch1–42 peptides were used as markers (lanes 1–3). A $\beta$  levels did not reach detection levels in predepositing APPDutch mice without immunoprecipitation (shown are 13-month-old mice). In contrast, in a 23-month-old amyloid depositing APPDutch mouse, A $\beta$ Dutch1–40, but not A $\beta$ Dutch1–42, was readily detected (lane 7). (d) Immunohistochemical analysis of a 29-month-old APPDutch mouse shows A $\beta$  deposition largely confined to leptomeningeal and neocortical vessels (NT12 antibody). No compact parenchymal deposits were seen. (e,f) Immunolabeling of vascular amyloid with antibodies specific to A $\beta$ 40 (R208 in e) and A $\beta$ 42 (R306 in f) reveals that the majority of vascular amyloid ends at amino acid 40. (g) Congo red staining of amyloid-laden vessels demonstrates that the vast majority of the amyloid is of compact nature and congophilic. (h) High-magnification view of amyloid-containing cortical vessels that shows a vessel-within-vessel configuration. (i) Electron micrograph demonstrating abundant amyloid fibrils (asterisk) between the smooth muscle cells (SMC) in a 30-month-old APPDutch mouse. Scale bars are 1 mm (a), 10  $\mu$ m (b, e–h), 200  $\mu$ m (d) and 1  $\mu$ m (i).



deposits revealed the presence of both A $\beta$ wt1–40 and A $\beta$ wt1–42, whereas in APPDutch mice, A $\beta$ Dutch1–40 was seen but A $\beta$ Dutch1–42 was below detection level (Fig. 4b). This was confirmed by ELISA, which revealed a more than fourfold higher human A $\beta$ 40/A $\beta$ 42 ratio in APPDutch mice than in APPwt mice (Table 1; for absolute values, see Supplementary Table 1 online). We also analyzed steady-state levels of A $\beta$ 40 and A $\beta$ 42 in APPDutch and APPwt mice at 7 months, before detectable amyloid deposition, to determine whether this difference in the ratio of A $\beta$ 40 to A $\beta$ 42 is an early event or is only seen after the accumulation of amyloid. An almost twofold greater A $\beta$ 40/A $\beta$ 42 ratio was seen in young APPDutch mice than in APPwt mice of similar age (Table 1 and Supplementary Table 1).

#### Massive parenchymal amyloid in APPDutch/PS45 mice

Examining our hypothesis that a high ratio of A $\beta$ Dutch1–40 to A $\beta$ Dutch1–42 is linked to and potentially necessary for the predomi-

nant vascular amyloid deposition in APPDutch mice, we crossed APPDutch mice with mice that overexpress human presenilin-1 (PS1) bearing the G384A mutation (PS45 mice). This mutation is known to increase A $\beta$ 1–42 production<sup>16,17</sup>. Notably, starting at 12 weeks of age, APPDutch/PS45 double-transgenic mice developed parenchymal amyloid in the neocortex and hippocampus. At 10 months, massive diffuse and compact parenchymal amyloid was found in virtually all brain regions. Unlike in the APPDutch mice, vascular amyloid, although present, was a much less prominent feature in the APPDutch/PS45 mice (Fig. 5a).

Western blot analysis of APPDutch/PS45 brain homogenates revealed abundant A $\beta$ Dutch1–42 in addition to A $\beta$ Dutch1–40 (Fig. 5b). ELISA measurements confirmed this observation, with A $\beta$ Dutch42 at least twice as abundant as A $\beta$ Dutch40 in double-transgenic mice, both before (predepositing) and after (depositing) the onset of amyloid deposition (Table 1 and Supplementary Table 1). These results demonstrate that A $\beta$ Dutch is capable of forming parenchymal amyloid deposits and that

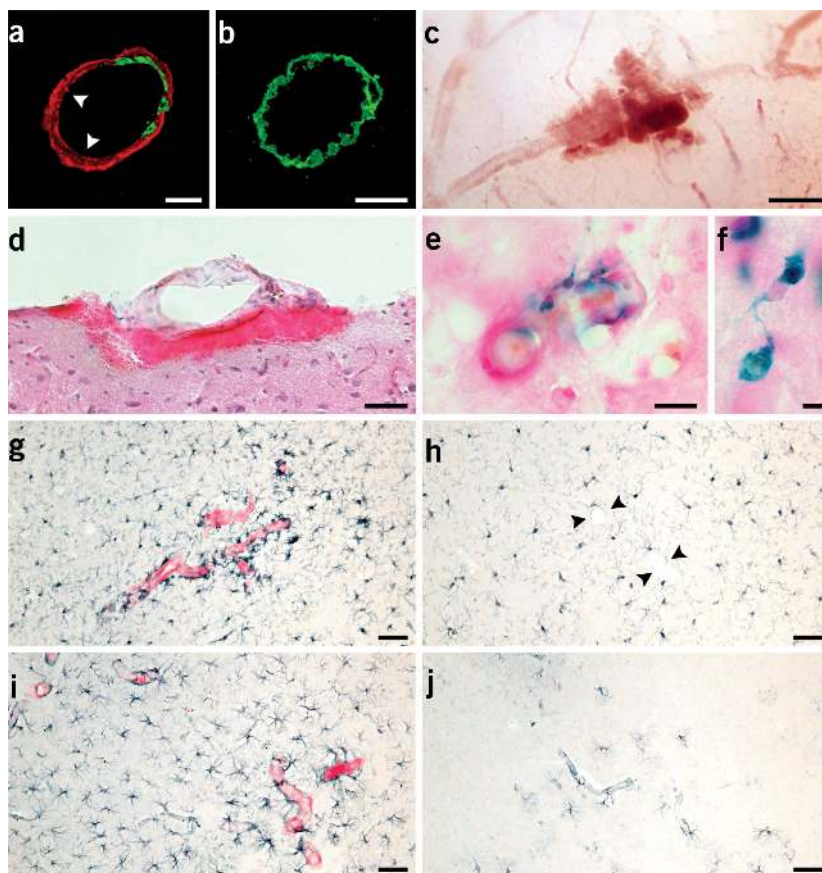


**Figure 3** Hemorrhages and neuroinflammation in APPDutch mice. **(a)** Double labeling for smooth muscle cell actin (green) and A $\beta$  (red) in a leptomeningeal vessel of a 29-month-old APPDutch mouse reveals displacement of smooth muscle cells by vascular amyloid (arrowheads). **(b)** Vessels that are not affected by A $\beta$  show a continuous rim of smooth muscle cells. Shown are superpositions of optical sections. **(c)** A fresh hemorrhage is shown that occurred at the surface of the brain of a 29-month-old APPDutch mouse. **(d)** Hematoxylin and eosin (H&E) staining on a cross-section through the bleeding shown in **c**. **(e)** Microhemorrhage associated with amyloid-laden vessels visualized by Perls' Prussian blue staining for ferric iron. **(f)** High magnification of such microbleeds reveal hemosiderin-positive microglia. **(g)** Activated perivascular microglia (blue) in the immediate vicinity of amyloid-laden vessels (Congo red) in the neocortex of a 29-month-old APPDutch mouse. **(h)** Such microgliosis was absent in the same mouse around unaffected vessels (arrowheads). **(i)** Reactive astrocytes (blue) in neocortical areas with CAA (Congo red). **(j)** In neocortical regions with no vascular amyloid, no reactive astrocytes were observed. Scale bars are 20  $\mu$ m (**a,b,e**), 100  $\mu$ m (**c,g-j**), 50  $\mu$ m (**d**) and 5  $\mu$ m (**f**).

such deposits can be induced in APPDutch mice by increasing the production of A $\beta$ Dutch42 via the expression of mutant presenilin.

#### Endogenous murine A $\beta$ is codeposited with human A $\beta$

To determine whether endogenous murine A $\beta$ , the counterpart of A $\beta$ wt derived from the wild-type allele in individuals with HCHWA-D, is codeposited with transgene-derived human A $\beta$  in APPDutch mice, we used ELISA specific for murine A $\beta$ 40 and A $\beta$ 42. The amount of murine A $\beta$  was  $4.4 \pm 0.1\%$  of the human A $\beta$  detected in APPwt mice and  $8.0 \pm 1.0\%$  of that detected in APPDutch mice. Notably, depositing APPDutch mice showed a roughly threefold higher ratio of murine A $\beta$ 40 to A $\beta$ 42 than was seen in APPwt mice (Table 1 and Supplementary Table 1).

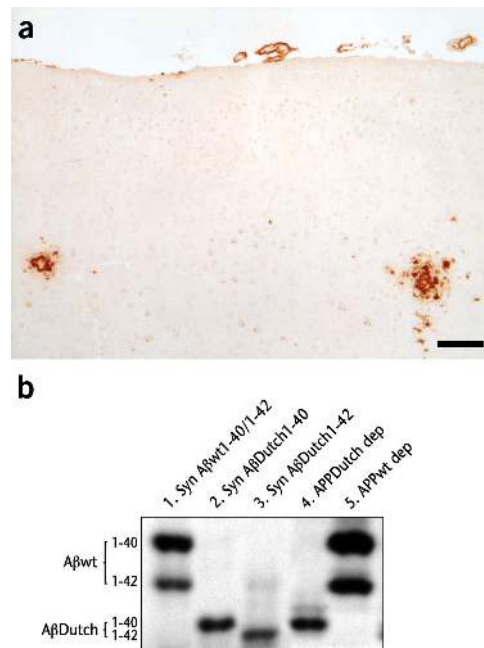
#### DISCUSSION

Although the APP mutation that causes HCHWA-D was identified more than a decade ago<sup>4</sup>, progress toward understanding the pathogenesis of HCHWA-D has been hampered by the absence of an animal model. Here we describe a transgenic mouse model that develops extensive cerebrovascular amyloid deposits in leptomeningeal and cortical vessels, similar to those found in affected people<sup>5,7</sup>. Parenchymal amyloid is nearly absent in these transgenic mice, and the few parenchymal plaques found are diffuse. The observation that neuronal expression of APPDutch is sufficient for cerebrovascular amyloidosis, smooth muscle cell degeneration and hemorrhage in a mouse model strongly suggests that neurons are the source of the cerebrovascular amyloid in HCHWA-D. Moreover, these results demonstrate that smooth muscle cell degeneration does not require intracellular A $\beta$  production but can be initiated by extracellular, neuron-derived A $\beta$  that is transported to and accumulates at the vasculature.

Expanding on previous research<sup>18,19</sup>, we found that amyloid deposits in human HCHWA-D brains contain not only A $\beta$ Dutch40 but also abundant A $\beta$ wt40, with only little A $\beta$ 42. In the APPDutch mice, as in human HCHWA-D, the vast majority of the deposited A $\beta$  is A $\beta$ 40, with roughly 12 times more A $\beta$ Dutch40 than A $\beta$ Dutch42. This is in contrast to the peptide ratios found in human AD and in APPwt mice or other transgenic mice expressing Swedish APP, where significantly more A $\beta$ 42 relative to A $\beta$ 40 is deposited<sup>20–23</sup>. In both HCHWA-D brain tissue and APPDutch mice, A $\beta$ wt derived from the wild-type allele in HCHWA-D and from the endogenous murine APP in the APPDutch mice followed the deposition pattern of the mutated A $\beta$ Dutch species.

The two other mouse models we have examined in this study further highlight the important role of the A $\beta$ 40/A $\beta$ 42 ratio in determining vascular versus parenchymal amyloid deposition. APPwt mice overexpressed APP at levels comparable to APPDutch mice, but the former developed abundant parenchymal plaques and only sparse vascular amyloidosis, suggesting that the single E693Q amino acid substitution is sufficient to target neuron-derived A $\beta$  to the vessel wall. Notably, the A $\beta$ 40/A $\beta$ 42 ratio was significantly lower in APPwt mice than in APPDutch mice. Thus, a straightforward explanation for why the Dutch mutation leads to CAA could be that it favors the production of A $\beta$ 40, which in turn is vasculotropic. To examine this hypothesis, we determined the A $\beta$ 40/A $\beta$ 42 ratio in young transgenic mice before the onset of amyloid deposition, where a twofold higher ratio of A $\beta$ 40/A $\beta$ 42 was seen in APPDutch mice than in APPwt mice. In conditioned media of E693Q transfected cells, a similar, albeit somewhat smaller, increase in the A $\beta$ 40/A $\beta$ 42 ratio has been reported<sup>11,24</sup>. This suggests that the Dutch mutation affects A $\beta$ 40/A $\beta$ 42 ratios at the level of A $\beta$  production or clearance. Recent results show that A $\beta$ Dutch40 is more resistant to proteolysis by both neprilysin and insulin-degrading enzyme<sup>25,26</sup> and is less efficiently cleared into the blood<sup>13</sup> than A $\beta$ wt40. Similar studies with A $\beta$ Dutch42, however, have not been reported.

**Figure 4** Parenchymal and vascular amyloid deposition in APPwt mice. (a) A $\beta$ -immunostaining of an 18-month-old APPwt mouse reveals parenchymal amyloid deposits with only scattered CAA. (b) Western blot analysis of human A $\beta$  in APPwt brain in comparison to APPDutch brain. Lanes 1–3, synthetic human A $\beta$ . In amyloid-depositing APPwt mice (18 months), a substantial A $\beta$ wt1–40 and a somewhat weaker A $\beta$ wt1–42 band were observed (lane 5), whereas in amyloid-depositing APPDutch mice (23 months), only A $\beta$ Dutch1–40 was detected (lane 4). Scale bar is 100  $\mu$ m.



Familial AD-causing PS1 mutations shift the generation of A $\beta$  to favor A $\beta$ 42, which results in early and robust parenchymal amyloid deposition in transgenic mice that produce human wild-type A $\beta$ <sup>16,27,28</sup>. Crossing the APPDutch mouse with the PS45 line resulted in abundant parenchymal plaque formation at a young age, with limited CAA pathology. Thus, although A $\beta$ Dutch preferentially accumulates around cerebral vessels, genetically shifting the A $\beta$ Dutch40/A $\beta$ Dutch42 ratio to favor A $\beta$ Dutch42 was sufficient to alter the distribution of the resulting amyloid pathology from the vasculature to the parenchyma. Moreover, this demonstrates that A $\beta$ Dutch can form dense and congophilic plaques within the parenchyma. Therefore, parenchymal amyloid formation in APPDutch mice and humans with HCHWA-D is likely to be limited by the absence of A $\beta$ 42-driven parenchymal amyloid seeding. The present data do not rule out a role for A $\beta$ 42 as seed for vascular amyloid<sup>29</sup>.

We have previously shown that cerebral amyloidosis is not a local process and that A $\beta$  can be transported extracellularly and accumulate distant to its site of production<sup>30</sup>, as must also occur in the APPDutch mouse. This observation, together with the finding of similar intraneuronal A $\beta$  accumulation in APPDutch and APPwt transgenic mice (Supplementary Fig. 1 online), indicate that different A $\beta$  species interact differently with the extracellular environment, making A $\beta$  movement through the different local environments in the CNS an important determinant of amyloid pathology. For instance, when A $\beta$ 42 concentration is insufficient to form and maintain parenchymal amyloid seeds, soluble A $\beta$  is transported from neurons to the vasculature, where it is cleared into the blood or drained along perivascular spaces<sup>31,32</sup>. Coupled with the observation that

A $\beta$ Dutch40 is less efficiently cleared than A $\beta$ wt40 is<sup>13</sup>, this may in part explain why A $\beta$ Dutch40 accumulates at the vessel wall in APPDutch mice, whereas it can accumulate within the parenchyma when these mice are crossed with PS45 mice.

The knowledge that both A $\beta$ 40 and A $\beta$ 42 have the potential to drive amyloid pathology, albeit within different compartments, will undoubtedly have further implications as anti-A $\beta$  therapies are developed. For example, anti-A $\beta$  immunotherapy has been shown to preferentially clear A $\beta$ 42 from mice with preexisting amyloid pathology<sup>33,34</sup>. Although selective clearance of A $\beta$ 42 would beneficially reduce parenchymal amyloid burden, this might potentiate vascular amyloid pathology, as has been alluded to in A $\beta$ -immunotherapy studies done in mice and may also have been the case for the two A $\beta$ 42-immunized human patients who have gone to autopsy<sup>33,35–37</sup>. Given this complexity, further studies of anti-A $\beta$  therapies will need to follow alterations in the A $\beta$ 40/A $\beta$ 42 ratio, while addressing the resulting balance of vascular and parenchymal amyloid pathology.

Most individuals with HCHWA-D die early due to recurrent strokes<sup>6</sup>, but some with relatively restricted stroke pathology reach a considerable age. Nevertheless, these individuals show a continuous cognitive decline similar to that seen in persons with AD<sup>38</sup>. This supports recent studies suggesting that CAA is not only a significant cause of intracerebral hemorrhage in the elderly but also an important contributing factor to cognitive impairment and AD dementia<sup>39</sup>. CAA may interfere with the anatomical integrity of the vessel wall and the physio-

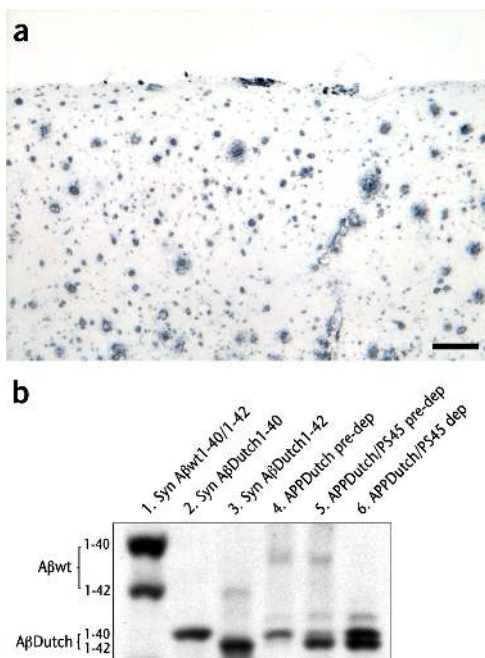


**Figure 5** Predominant parenchymal amyloid deposition in APPDutch/PS45 double-transgenic mice. (a) A $\beta$ -immunostaining of a 10-month-old APPDutch/PS45 mouse shows extensive, predominantly diffuse, but also some congophilic, parenchymal amyloid deposits with only scattered CAA. (b) Western blot analysis of human A $\beta$  in mouse brain immunoprecipitates. Lanes 1–3, synthetic human A $\beta$ . Predepositing (4-month-old) APPDutch mouse reveals only A $\beta$ Dutch1–40 (lane 4). In contrast, both A $\beta$ Dutch1–40 and 1–42 were detectable in a predepositing 2.5-month-old APPDutch/PS45 mouse (lane 5) and a depositing 10-month-old APPDutch/PS45 mouse (lane 6). In order to show A $\beta$ Dutch1–40 and 1–42 as distinct bands, the sample shown in lane 6 was highly diluted. Scale bar is 100  $\mu$ m.



logical response to vasodilation, and it can occlude affected vessels and thus induce perivascular ischemia<sup>8,40,41</sup>. However, previous studies have been limited by their reliance on end-stage human autopsy cases and transgenic models that have severe parenchymal amyloidosis in addition to CAA<sup>40–43</sup>. Our APPDutch model, which recapitulates well human HCHWA-D, is likely to be a useful tool for the further study of the pathogenic mechanisms by which CAA affects cognition and neurodegeneration, as well as for the development of therapeutic strategies.

## METHODS

**Human patients.** Tissue of frontal cortex and pial vessels was obtained at autopsy from five HCHWA-D patients (50–76 years of age; postmortem delay 5–48 h). For comparison, cortical tissue from nine individuals with autopsy-confirmed AD (61–93 years of age, postmortem delay 4–26 h) and two control individuals (78 and 87 years of age, postmortem delay 4–11 h) was used.

**Generation of transgenic mice.** To generate Dutch-mutant APP transgenic mice, human APP751 cDNA with the E693Q mutation was inserted into the blunt-ended *XhoI* site of the vector pTSC $\alpha$ 1 containing the murine *Thy1.2* minigene<sup>44</sup>. After removal of vector sequences by *NotI/PvuI* digestion, linear Thy1-APP constructs were injected into C57BL/6J oocytes. Five positive transgenic founder mice (C57BL/6J-TgN(Thy1-APP<sub>E693Q</sub>)) were identified and expression of human APP was assessed by western blot and immunohistochemistry. The two lines with the highest transgene expression (lines 23 and 33) were used in this study (APPDutch mice). Expression levels in these lines are about five times greater than endogenous APP levels (data not shown). The generation of the wild-type human APP751 transgenic mice (C57BL/6J-TgN(Thy1-APP)51) has been described previously<sup>45</sup>. Line 16 (APPwt mice), which has a similar or slightly higher APP expression level than the APPDutch mice, was used in this study. APPDutch/PS45 double-transgenic mice were obtained by crossing APPDutch mice with mice overexpressing human G384A-mutated presenilin-1 (PS1) under the control of the murine Thy1 promoter (B6,D2-TgN(Thy1-PS1<sub>G384A</sub>)45). These PS45 mice were backcrossed to C57BL/6J for more than seven generations prior to use. All mice analyzed were hemizygous for the transgene(s) of interest. All animal experiments were in compliance with protocols approved by the local Animal Care and Use Committees.

**Histology and immunohistochemistry.** Tissue was immersion-fixed in 4% paraformaldehyde. Histology and immunohistochemistry were done on either 4- $\mu$ m-thick paraffin-embedded sections or 25- $\mu$ m-thick free-floating frozen sections. A $\beta$  was immunostained with rabbit polyclonal antibody NT12 (NT11), gifts of P. Paganetti (Basel, Switzerland)<sup>44</sup> using standard immunoperoxidase procedures with Elite ABC kits (Vector Laboratories), with 3,3'-diaminobenzidine (Sigma) or Vector SG (Vector Laboratories) as substrates. For specific staining of A $\beta$ <sub>x-40</sub> or A $\beta$ <sub>x-42</sub>, we used rabbit antisera R208 (R163) or R306 (R165), respectively<sup>46</sup> (gift of P. Mehta, New York). All A $\beta$  antibodies recognized both A $\beta$ wt and A $\beta$ Dutch. Human APP (hAPP) was visualized with polyclonal antibody A4CT (specific to the C-terminal 100 amino acids of APP; courtesy of K. Beyreuther, Heidelberg, Germany). Microglia and astroglia were stained with rabbit polyclonal antibody to ionized calcium binding adaptor molecule-1 (Iba-1)<sup>47</sup> (courtesy of Y. Imai, Tokyo) and rabbit polyclonal antibody to glial fibrillary acidic protein (Dako), respectively. Double immunofluorescence labeling of A $\beta$  and smooth muscle cells was done for confocal microscopy. NT12 and mouse monoclonal antibody to  $\alpha$ -smooth muscle actin (A-2547, Sigma) followed by goat anti-rabbit Alexa 568 and goat anti-mouse Alexa 488 (Molecular Probes) were used. Staining with Congo red, Thioflavin S and Perls' Prussian blue reaction for ferric iron was done according to standard protocols<sup>41</sup>.

**Electron microscopy.** Mice were perfused with ice-cold PBS for 5 min. Neocortical tissue pieces were removed and immersion-fixed in 4% paraformaldehyde and 0.5% glutaraldehyde at 4 °C. The tissue was then postfixed in 1% osmium tetroxide in 0.1 M cacodylate buffer, dehydrated, and then processed for Spurr embedding. Ultrathin sections were cut from selected areas, stained with uranyl acetate and lead citrate, and then examined and photographed with a Jeol JEM1011 electron microscope.

**In situ hybridization.** *In situ* hybridization for human APP was done as previously described<sup>44</sup>. In brief, a <sup>33</sup>P-labeled oligonucleotide probe, 5'-AGC-CTCTTCTCTACCTCATCACCATCCTCATCGTCTCG-3', complementary to the coding sequence of hAPP between nucleotides 859 and 898, was used at a final concentration of 2 pmol/ml.

**Western blot analysis.** APP expression levels in transgenic mice were analyzed using standard 8% SDS-polyacrylamide minigels followed by blotting and antibody binding as described below. For analysis of A $\beta$ , we used western blots as previously described<sup>15</sup>. Briefly, samples of homogenized brain hemispheres were subjected to SDS-PAGE using 10% T, 5% C bicine/Tris minigels containing 8 M urea in the separation gel. To detect A $\beta$  in brains of predepositing mice, we used immunoprecipitation with antibody 6E10. Proteins were transferred to a PVDF Immobilon-P membrane (Millipore) by semi-dry blotting, incubated with antibody 6E10 (Signet) and visualized by chemiluminescence (ECL, Amersham). Antibody 6E10 recognizes residues 1–17 of A $\beta$ , and the Dutch mutation at position 22 does not interfere with its binding. Synthetic A $\beta$ wt1–40 and A $\beta$ wt1–42 peptides were purchased from Bachem. Synthetic A $\beta$ Dutch species were gifts of J. Ghiso (New York), G. Labeur (Ghent, Belgium) and W. E. Van Nostrand (Stony Brook, New York, USA).

**ELISA.** Cerebral A $\beta$  levels of patients and A $\beta$ -depositing mice were assayed by sandwich ELISA from formic acid-extracted sucrose homogenates prepared from postmortem human cortical tissue or mouse hemi-brains lacking the cerebellum, as previously described<sup>48</sup>. A $\beta$  was captured with A $\beta$  C-terminal monoclonal antibodies that recognize exclusively either A $\beta$ <sub>x-40</sub> (JRF/cA $\beta$ 40/10) or A $\beta$ <sub>x-42</sub> (JRF/cA $\beta$ 42/26) and are detected with horseradish peroxidase-conjugated JRF/A $\beta$ tot/17, which is specific to the N-terminal 16 residues of human A $\beta$ <sup>48</sup>. A $\beta$  levels in mice prior to amyloid deposition were determined by preparing a sucrose homogenate from each hemisphere (without cerebellum) and then extracting this in diethylamine (DEA), as previously described<sup>49</sup>. Endogenous murine A $\beta$  was similarly detected using DEA extraction and a murine-specific monoclonal antibody for detection (JRF/rA $\beta$ 1-15/2)<sup>49</sup>. ELISA results are reported as the mean  $\pm$  s.e.m. in pmol A $\beta$  per gram of wet brain, based on standard curves using synthetic A $\beta$ 1–40 and A $\beta$ 1–42 peptide standards (American Peptide). The values were compared by non-parametric Mann-Whitney *U* tests. All capture and detection antibodies were a gift from M. Mercken (Johnson and Johnson Pharmaceutical Research and Development/Janssen Pharmaceutica).

*Note: Supplementary information is available on the Nature Neuroscience website.*

## ACKNOWLEDGMENTS

We would like to thank H. Widmer for experimental help; L. Walker, J. Ghiso and T. Saido for comments on this manuscript; and R. Nixon for support of the ELISA measurements. This work was supported by grants to M.J. from the Fritz Thyssen Foundation (Cologne, Germany), the EU under the sixth framework programme (priority: life sciences and health, LSHM-CT-2003-503330) and the Swiss National Science Foundation. This work was also supported by grants to P.M.M. from the National Institute on Aging and the National Institute of Neurological Disorders and Stroke.

## COMPETING INTERESTS STATEMENT

The authors declare that they have no competing financial interests.

Received 15 March; accepted 12 July 2004

Published online at <http://www.nature.com/natureneuroscience/>

- Haass, C. & Steiner, H. Protofibrils, the unifying toxic molecule of neurodegenerative disorders? *Nat. Neurosci.* **4**, 859–860 (2001).
- Hardy, J. Amyloid, the presenilins and Alzheimer's disease. *Trends. Neurosci.* **20**, 154–159 (1997).
- Selkoe, D.J. Translating cell biology into therapeutic advances in Alzheimer's disease. *Nature* **399**, A23–31 (1999).
- Levy, E. *et al.* Mutation of the Alzheimer's disease amyloid gene in hereditary cerebral hemorrhage, Dutch type. *Science* **248**, 1124–1126 (1990).
- Wattendorff, A.R., Bots, G.T., Went, L.N. & Endtz, L.J. Familial cerebral amyloid angiopathy presenting as recurrent cerebral haemorrhage. *J. Neurol. Sci.* **55**, 121–135 (1982).
- Bornebroek, M., Haan, J., Maat-Schieman, M.L., Van Duinen, S.G. & Roos, R.A. Hereditary cerebral hemorrhage with amyloidosis-Dutch type (HCHWA-D). I. A review of clinical, radiologic and genetic aspects. *Brain. Pathol.* **6**, 111–114 (1996).

7. Maat-Schieman, M.L., van Duinen, S.G., Bornebroek, M., Haan, J. & Roos, R.A. Hereditary cerebral hemorrhage with amyloidosis-Dutch type (HCHWA-D). II. A review of histopathological aspects. *Brain Pathol.* **6**, 115–120 (1996).
8. Vinters, H.V. Cerebral amyloid angiopathy. A critical review. *Stroke* **18**, 311–324 (1987).
9. Greenberg, S.M. Cerebral amyloid angiopathy: prospects for clinical diagnosis and treatment. *Neurology* **51**, 690–694 (1998).
10. Fraser, P.E. *et al.* Fibril formation by primate, rodent, and Dutch-hemorrhagic analogues of Alzheimer amyloid  $\beta$ -protein. *Biochemistry* **31**, 10716–10723 (1992).
11. De Jonghe, C. *et al.* Flemish and Dutch mutations in amyloid  $\beta$  precursor protein have different effects on amyloid  $\beta$  secretion. *Neurobiol. Dis.* **5**, 281–286 (1998).
12. Watson, D.J., Selkoe, D.J. & Teplow, D.B. Effects of the amyloid precursor protein Glu693 $\Delta$ E $\Delta$ Gln 'Dutch' mutation on the production and stability of amyloid  $\beta$ -protein. *Biochem. J.* **340** (Pt 3), 703–709 (1999).
13. Monro, O.R. *et al.* Substitution at codon 22 reduces clearance of Alzheimer's amyloid- $\beta$  peptide from the cerebrospinal fluid and prevents its transport from the central nervous system into blood. *Neurobiol. Aging* **23**, 405–412 (2002).
14. Van Nostrand, W.E., Melchor, J.P. & Ruffini, L. Pathologic amyloid  $\beta$ -protein cell surface fibril assembly on cultured human cerebrovascular smooth muscle cells. *J. Neurochem.* **70**, 216–223 (1998).
15. Klafki, H.W., Wiltfang, J. & Staufenbiel, M. Electrophoretic separation of  $\beta$ A4 peptides (1–40) and (1–42). *Anal. Biochem.* **237**, 24–29 (1996).
16. Citron, M. *et al.* Mutant presenilins of Alzheimer's disease increase production of 42-residue amyloid  $\beta$ -protein in both transfected cells and transgenic mice. *Nat. Med.* **3**, 67–72 (1997).
17. De Jonghe, C. *et al.* Evidence that A $\beta$ 42 plasma levels in presenilin-1 mutation carriers do not allow for prediction of their clinical phenotype. *Neurobiol. Dis.* **6**, 280–287 (1999).
18. Castano, E.M. *et al.* The length of amyloid- $\beta$  in hereditary cerebral hemorrhage with amyloidosis, Dutch type. Implications for the role of amyloid- $\beta$  1–42 in Alzheimer's disease. *J. Biol. Chem.* **271**, 32185–32191 (1996).
19. Prelli, F. *et al.* Expression of a normal and variant Alzheimer's  $\beta$ -protein gene in amyloid of hereditary cerebral hemorrhage, Dutch type: DNA and protein diagnostic assays. *Biochem. Biophys. Res. Commun.* **170**, 301–307 (1990).
20. Jankowsky, J.L. *et al.* Mutant presenilins specifically elevate the levels of the 42 residue  $\beta$ -amyloid peptide in vivo: evidence for augmentation of a 42-specific  $\gamma$ -secretase. *Hum. Mol. Genet.* **13**, 159–170 (2004).
21. Johnson-Wood, K. *et al.* Amyloid precursor protein processing and A $\beta$ 42 deposition in a transgenic mouse model of Alzheimer disease. *Proc. Natl. Acad. Sci. USA* **94**, 1550–1555 (1997).
22. Richards, J.G. *et al.* PS2APP transgenic mice, coexpressing hPS2mut and hAPP<sup>swe</sup>, show age-related cognitive deficits associated with discrete brain amyloid deposition and inflammation. *J. Neurosci.* **23**, 8989–9003 (2003).
23. Hsiao, K. *et al.* Correlative memory deficits, A $\beta$  elevation, and amyloid plaques in transgenic mice. *Science* **274**, 99–102 (1996).
24. Nilsberth, C. *et al.* The 'Arctic' APP mutation (E693G) causes Alzheimer's disease by enhanced A $\beta$  protofibril formation. *Nat. Neurosci.* **4**, 887–893 (2001).
25. Tsubuki, S., Takaki, Y. & Saido, T.C. Dutch, Flemish, Italian, and Arctic mutations of APP and resistance of A $\beta$  to physiologically relevant proteolytic degradation. *Lancet* **361**, 1957–1958 (2003).
26. Morelli, L. *et al.* Differential degradation of amyloid  $\beta$  genetic variants associated with hereditary dementia or stroke by insulin-degrading enzyme. *J. Biol. Chem.* **278**, 23221–23226 (2003).
27. Borchelt, D.R. *et al.* Accelerated amyloid deposition in the brains of transgenic mice coexpressing mutant presenilin 1 and amyloid precursor proteins. *Neuron* **19**, 939–945 (1997).
28. Holcomb, L. *et al.* Accelerated Alzheimer-type phenotype in transgenic mice carrying both mutant amyloid precursor protein and presenilin 1 transgenes. *Nat. Med.* **4**, 97–100 (1998).
29. Natta, R. *et al.* Ultrastructural evidence of early non-fibrillar A $\beta$ 42 in the capillary basement membrane of patients with hereditary cerebral hemorrhage with amyloidosis, Dutch type. *Acta Neuropathol. (Berl.)* **98**, 577–582 (1999).
30. Meyer-Luehmann, M. *et al.* Extracellular amyloid formation and associated pathology in neural grafts. *Nat. Neurosci.* **6**, 370–377 (2003).
31. Shibata, M. *et al.* Clearance of Alzheimer's amyloid- $\beta$ (1–40) peptide from brain by LDL receptor-related protein-1 at the blood-brain barrier. *J. Clin. Invest.* **106**, 1489–1499 (2000).
32. Weller, R.O. *et al.* Cerebral amyloid angiopathy: amyloid  $\beta$  accumulates in putative interstitial fluid drainage pathways in Alzheimer's disease. *Am. J. Pathol.* **153**, 725–733 (1998).
33. Pfeifer, M. *et al.* Cerebral hemorrhage after passive anti-A $\beta$  immunotherapy. *Science* **298**, 1379 (2002).
34. Das, P., Murphy, M.P., Younkin, L.H., Younkin, S.G. & Golde, T.E. Reduced effectiveness of A $\beta$ 1–42 immunization in APP transgenic mice with significant amyloid deposition. *Neurobiol. Aging* **22**, 721–727 (2001).
35. Nicoll, J.A. *et al.* Neuropathology of human Alzheimer disease after immunization with amyloid- $\beta$  peptide: a case report. *Nat. Med.* **9**, 448–452 (2003).
36. Koller, M.F. *et al.* Active immunization of mice with an A $\beta$ -Hsp70 vaccine. *Neurodegenerative Dis.* **1**, 20–28 (2004).
37. Ferrer, I., Boada Rovira, M., Sánchez Guerra, M.L., Rey, M.J. & Costa-Jussà, F. Neuropathology and pathogenesis of encephalitis following amyloid- $\beta$  immunization in Alzheimer's disease. *Brain Pathol.* **14**, 11–20 (2004).
38. Natta, R. *et al.* Dementia in hereditary cerebral hemorrhage with amyloidosis-Dutch type is associated with cerebral amyloid angiopathy but is independent of plaques and neurofibrillary tangles. *Ann. Neurol.* **50**, 765–772 (2001).
39. Greenberg, S.M. Cerebral amyloid angiopathy and dementia: two amyloids are worse than one. *Neurology* **58**, 1587–1588 (2002).
40. Christie, R., Yamada, M., Moskowitz, M. & Hyman, B. Structural and functional disruption of vascular smooth muscle cells in a transgenic mouse model of amyloid angiopathy. *Am. J. Pathol.* **158**, 1065–1071 (2001).
41. Winkler, D.T. *et al.* Spontaneous hemorrhagic stroke in a mouse model of cerebral amyloid angiopathy. *J. Neurosci.* **21**, 1619–1627 (2001).
42. Calhoun, M.E. *et al.* Neuronal overexpression of mutant amyloid precursor protein results in prominent deposition of cerebrovascular amyloid. *Proc. Natl. Acad. Sci. USA* **96**, 14088–14093 (1999).
43. Van Dorpe, J. *et al.* Prominent cerebral amyloid angiopathy in transgenic mice overexpressing the london mutant of human APP in neurons. *Am. J. Pathol.* **157**, 1283–1298 (2000).
44. Sturchler-Pierrat, C. *et al.* Two amyloid precursor protein transgenic mouse models with Alzheimer disease-like pathology. *Proc. Natl. Acad. Sci. USA* **94**, 13287–13292 (1997).
45. Bodendorf, U. *et al.* Expression of human  $\beta$ -secretase in the mouse brain increases the steady-state level of  $\beta$ -amyloid. *J. Neurochem.* **80**, 799–806 (2002).
46. Mehta, P.D. *et al.* Plasma and cerebrospinal fluid levels of amyloid  $\beta$  proteins 1–40 and 1–42 in Alzheimer disease. *Arch. Neurol.* **57**, 100–105 (2000).
47. Ohsawa, K., Imai, Y., Kanazawa, H., Sasaki, Y. & Kohsaka, S. Involvement of Iba1 in membrane ruffling and phagocytosis of macrophages/microglia. *J. Cell. Sci.* **113** (Pt 17), 3073–3084 (2000).
48. Janus, C. *et al.* A $\beta$  peptide immunization reduces behavioural impairment and plaques in a model of Alzheimer's disease. *Nature* **408**, 979–982 (2000).
49. Rozmahel, R. *et al.* Normal brain development in PS1 hypomorphic mice with markedly reduced  $\gamma$ -secretase cleavage of  $\beta$ APP. *Neurobiol. Aging* **23**, 187–194 (2002).
50. Maat-Schieman, M.L., Yamaguchi, H., van Duinen, S.G., Natta, R. & Roos, R.A. Age-related plaque morphology and C-terminal heterogeneity of amyloid  $\beta$  in Dutch-type hereditary cerebral hemorrhage with amyloidosis. *Acta Neuropathol. (Berl.)* **99**, 409–419 (2000).